Ain Shams Engineering Journal (2014) 5, 333–341

Ain Shams University

Ain Shams Engineering Journal

www.elsevier.com/locate/asej
www.sciencedirect.com

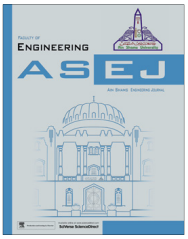

CIVIL ENGINEERING

Local bed morphological changes due to oriented groins in straight channels

M.M. Ibrahim *

Shoubra Faculty of Engineering, Benha University, PO Box 11629, Shoubra, Egypt

Received 24 September 2013; revised 23 November 2013; accepted 17 December 2013
Available online 22 January 2014

KEYWORDS

Morphological changes;
Groins;
Contraction ratio;
Orientation angle;
Scour;
Silting

Abstract This research investigates the effect of implementing oriented groins on the scour and silting processes in a straight channel. Combined physical and numerical models were used. Twenty-seven (27) runs were conducted in which the geometry of scour and silting associated with model groins was evaluated. Groin models were angled at 60°, 90°, and 120° to the downstream channel side wall with contraction ratios of 0.10, 0.15 and 0.20. The main goals of this paper were to evaluate the effect of the three angles on the scour geometry on minimizing erosion adjacent to the stream banks. Results were analyzed and were graphically presented and the percentages of errors between the obtained results from the used models were reported to define the sufficient compatibility between the used models. Simple formulae were derived to evaluate the scour and silting parameters.

1. Introduction

Groins may be defined as a structure extending outward from the bank of a stream for the purpose of deflecting the current away from the bank to protect it from erosion. Groins have also been used to enhance aquatic habitat by creating stable pools in unstable streams, Klingeman et al. [1]. Groins cause pools to be created and maintained, and have been found, in general, to be more beneficial to aquatic habitat resources than other types of bank protection. The magnitude of the benefit to the habitat in a disturbed stream is related to the volume of scour hole. Shields et al. [2] documented significant increases in fish numbers, size, biomass, and number of species in an incised stream following modification of groins to enlarge scour hole sand increase the percentage of pools in the reach. Designers of bank stabilization structures should, where possible, select groin geometry which stabilizes the bank and provides the largest scour volume subject to cost constraints. The initiation of local scour is associated with the increase in shear stress caused by the accelerating flow around the obstruction. The volume of local scour in the vicinity of a spur dike is difficult to estimate accurately, therefore, this research was initiated with the objective of investigating the influence of groin length, orientation angle and discharge on the characteristics of local scour and silting with in order to determine the optimum characteristics according to groin usage with

* Tel.: +20 12 250 09 723.
E-mail addresses: drmebraheem@yahoo.com, mohamed.ibrahim@-feng.bu.edu.eg.

Peer review under responsibility of Ain Shams University.

Production and hosting by Elsevier

2090-4479 © 2014 Production and hosting by Elsevier B.V. on behalf of Ain Shams University.
http://dx.doi.org/10.1016/j.asej.2013.12.006

Nomenclature

U	longitudinal surface velocity (m/s)
V	transverse surface velocity (m/s)
P	mean pressure (kg/m^2)
F_X	body force in X direction (kg m/s^2)
F_Y	body force in Y direction (kg m/s^2)
g	gravity acceleration (m/s^2)
d_{sc}	maximum scour depth (m)
y	depth of approaching flow (m)
L	groin length (m)
B	channel width (m)
d_{sc}	scour depth (m)
W_{sc}	scour width (m)
L_{sc}	scour length (m)
h_{sl}	silting depth (m)
W_{sl}	silting width (m)
L_{sl}	silting length (m)
$Fr_{avr.cont}$	average Froude number at the contracted section (–)
Q	discharge (m^3/s)

Greek symbols

v_e	kinematics eddy viscosity (kg/m s)
ρ	fluid density (kg/m^3)
τ_{fx}	turbulent frictional stresses in X-direction (kg/m^2)
τ_{fy}	turbulent frictional stresses in Y-direction (kg/m^2)
θ	orientation angle (°)
σ_g	geometric standard deviation (–)

minimum side effects. The investigation phases are presented in this paper under the following headlines.

- Reviewing the literature
- Executing experimental work
- Modeling the problem in hand
- Analyzing and presenting the results
- Deducing formulas to evaluate the scour and silting parameters

2. Reviewing the literature

Many factors affecting the geometries of scour and silting around groins (i.e. length, alignment, flow intensity, shape, sediment size, and flow depth) are evident. Few studies have been made which investigated the morphological bed changes associated with oriented groins. Many researchers have studied the hydraulics of groins. Studies to date have predominantly investigated, local scour (Kuhnle et al. [3], Ohmoto and Hirakawa [4], Elawady et al. [5,6]), flow structure (Tominaga et al. [7], Uittewaal and Berg [8]) and the mass exchange in the groin fields (Uittewaal et al. [9]).

Abdelmageed [10] developed a relationship between the maximum and minimum velocities before and after installing oriented groin. Moreover, he reported that the maximum scour length and depth occurred for groin with 20% of aspect ratio. Ibrahim [11] used 2D flume model for measuring the velocity distribution associated with spur dikes and scour holes to define the influence of groin length and orientation angle. He indicated that the groin length is directly proportional to velocity at the groin field. Vaghefi et al. [12] investigated the geometry of the scour hole and topography of the bed around a T-shaped non-submerged spur dike located in a 90° bend. They developed a new equation for scour parameters at a T-shaped spur dike. Jamieson et al. [13] performed a series of laboratory flume experiments to study the effect of groins on flow field dynamics and sediment erosion in a 135° mobile-bed channel bend. They concluded that the outer bank region (particularly between groins) may still be at risk of erosion. Jamieson et al. [14] studied experimentally the flow field and sediment dynamics in a mobile-bed channel bend with and without the presence of stream barbs (upstream-angled submerged groins). They found that the vortices increased in the outer bank scour zone for all runs with and without barbs. Huthoff et al. [15] proved that the wing dike construction leads to water level lowering for in-bank flows and to water level increases for outer-bank (flood) flows. Ali and Uijttewaal [16] carried out experimental study to estimate and parameterize the form drag due to vegetated groin obstacle. They measured the energy head losses for a range of discharges and downstream water levels covering submerged and subcritical flow conditions. Uijttewaal [17] studied experimentally the effects of groin layout on the flow near the groin field For different types (i.e., standard reference groins, groins with a head having a gentle slope and extending into the main channel, permeable groins consisting of pile rows, and hybrid groins consisting of a lowered impermeable groin with a pile row on top). The study demonstrated that the turbulence properties near and downstream of the groin can be manipulated by changing the permeability and slope of the groin head. He also observed that for submerged conditions the flow becomes complex and locally dominated by three-dimensional effects. Fang et al. [18] used the large eddy simulation (LES) to investigate the influence of groin parameters (i.e., head shape, aspect ratio L/D, and length L) on the flow properties. They indicated that the rectangular groin generates higher turbulence intensities and larger vortices than a round-headed groin. Also, Eddies are formed at the groin tips and transported downstream. Sukhodolov et al. [19] studied the sediment distributions in a groin field. They found the concentration of suspended particulate matter reduces with distance from the shear layer toward the internal parts of the groin field. Maleki et al. [20] studied numerically the three-dimensional simulation of flow and vortex patterns around L-shaped impermeable groins at five different angles. They found that the maximum and minimum erosion are located at angles of 75° and 90° respectively. Naghshine et al. [21] studied the effect of groin angle on controlling the sediments entering the intake branching from a 180° bend. They deduced that groin with angle 90 degree showed the best potential for reducing sediment movement into division. Attia et al. [22] used 2D hydrodynamic model to investigate the effect of oblique spur dikes on the local study at Naga Hammadi Barrage. The study found that, the scour depth and length were directly proportional to orientation angle.

This research was thus initiated in order to investigate the influence of groin length, orientation angle and discharge on the characteristics of local scour and silting with the objectives of determining the optimum characteristics according to groin usage with minimum side effects. For this reason, a combination between experimental and two dimensional finite element numerical models Molinas and Hafez [23] and Ibrahim [24] was used.

3. Executing experimental work

All of the experiments were conducted in a flume located at the Hydraulics Research Institute experimental hall of the National Water Research Center, Egypt.

The flume channel is 40 m long, 0.4 m wide, 0.6 m deep, and the side walls along the entire length of the flume were made of glass with wood-frames. The horizontal bottom of the flume was made of ceramics and wood. The flume is associated with a steel wooden gate with an orifice with a rectangular shape, also has movable downstream gate that is located at the end of the flume. Centrifugal pump driven by induction motor to re-circulated the flow from an underground reservoir to the flume. The groin models were made of wood with a 0.6 m height and with different lengths 4, 6, and 8 cm. Model groins with three contraction ratios (10%, 15%, and 20%) and three angles (60°, 90° and 120°) were used in this study. The angle of the groin is defined as the angle between the downstream bank and the long axis of the dike. The tested discharges were 10, 20, and 30 l/s. A relatively uniform-sized sand covered 30 m of the channel bed in all of the experiments. The bed sediment had a median size of 0.58 mm and a geometric standard deviation ($\sigma_g = [(D_{84}/D_{16})^{0.5}]$ of 1.37.

3.1. Model set-up and measurement techniques

The following procedure was used for each experimental run. Before the experiment with the groin model in place, the sediment bed surface was leveled with a scraper blade mounted on a carriage that rode on the steel rods. After the bed was completely wetted and drained, a profile of the bed surface was collected with a mobile point gauge with an accuracy of $+0.1$ mm. The flume was then filled with water to obtain the desired depth. Before the pump was started an initial set of transects of the anticipated scour region was collected. Next, the pump was started and the discharge adjusted (ultrasonic flow-meter with an accuracy of $+1\%$). As soon as the flow rate in the channel was stable, the running time of the test is started. The experiments were all continued for at least 4 h. This time length 4 h was used as a practical time for comparison of the scour holes as the rate of change had decreased markedly. After 4 h, the pump was switched off and the flume is gradually drained. The bed topography was recorded using a precise mobile point gauge. On this basis, the effects of the far sidewall on the results of the experiments were assumed to be unimportant.

4. Modeling the problem in hand

The governing differential equations for the developed numerical model are in the Cartesian XY coordinates, along and across the main flow directions. On the other hand, the Navier Stokes equations are used to describe the motion. The fluid is assumed to be incompressible and follows a Newtonian shear stress law, whereby, viscous force is linearly related to the rate of strain. In the model, the hydrodynamics governing relationships are the equations of conservation of mass and momentum. Conservation of mass equation takes the form of the continuity equation while Newton's equations of motion in two dimensions express the conservation of momentum. The continuity equation is given as follows:

$$\frac{\partial U}{\partial X}+\frac{\partial V}{\partial Y}=0 \tag{1}$$

The momentum equation in the longitudinal (X) direction is as follows

$$U\frac{\partial U}{\partial X}+V\frac{\partial U}{\partial Y}=-\frac{1}{\rho}\frac{\partial P}{\partial X}+\frac{\partial}{\partial X}\left(2v_e\frac{\partial U}{\partial X}\right)+\frac{\partial}{\partial Y}\left(v_e\left(\frac{\partial U}{\partial Y}+\frac{\partial V}{\partial X}\right)\right)+F_X+\left(\frac{\partial}{\partial z}\left(\frac{\tau_{fx}}{\rho}\right)\right)Z=H \tag{2}$$

The momentum equation in the lateral (Y) direction is as follows

$$U\frac{\partial V}{\partial X}+V\frac{\partial V}{\partial Y}=-\frac{1}{\rho}\frac{\partial P}{\partial Y}+\frac{\partial}{\partial X}\left(v_e\left(\frac{\partial U}{\partial Y}+\frac{\partial V}{\partial X}\right)\right)+\frac{\partial}{\partial Y}\left(2v_e\frac{\partial V}{\partial Y}\right)+F_Y+\left(\frac{\partial}{\partial z}\left(\frac{\tau_{fy}}{\rho}\right)\right)Z=H \tag{3}$$

The assumptions of the hydrodynamic model are as follows:

- The density is constant (incompressible fluid);
- Flow conditions are constant;
- The turbulent viscosity varies with the velocity gradient;
- Surface is analyzed in a 2D;
- Free surface is a rigid lid;
- Pressure is hydrostatic; and
- Wind stresses are neglected.

It should be mentioned that complete details about numerical solution of the model governing equations, the boundary conditions, and the working flow chart were presented by Ibrahim [24].

4.1. Model runs

Twenty-seven experimental runs with different groin models are reported. The experiments were designed to vary the independent variables of bed shear velocity, flow depth, groin length, and groin angle. The run names were formulated as the first number refers to discharge. However, 3 letters were used S, A, and R for pointing to groin action on flow. The letter S refers to the straight groin (90°), A refers to attracting groin (60°), and the letter R refers to repelling groin (120°). The subtitle number refers to groin contraction ratio. For example $30A_{15}$ means the discharge 30 l/s, attracting groin of 60°, and 15% contraction ratio.

5. Analyzing and presenting the results

The results were emphasized on the influence of groin length, orientation angle, and discharge on local bed morphological changes. Fig. 1 shows preliminary description for location of

scour and silting associated with groin location with respect to flow direction.

5.1. Geometry of scour and silting

The volume of the scour holes increased with time in a similar manner for all the experiments. The shape and extent of the scour holes varied for the different angles of groins used in the experimental runs. The volume of scour and silting could not be quantified accurately due to the irregular geometry of bed morphological changes in the groin field, and the lab facilities, Fig. 12.

The maximum values for scour depths and silting heights, widths and lengths were measured by the point gauge and ordinary scale then reported in Table 1.

The maximum scour hole was found at longest repelling groin. However, the shortest attracting presents inconsiderable bed changes.

It is noticed that the used numerical model proved insufficient capability in predicting the values of width and length in terms of scour and silting with high accuracy.

The measured values were obtained from the experimental model; however the predicted ones were produced from the used numerical model. Through the investigation a good combination between the two used models was defined as the average percentage of errors (i.e. 6.447% and 6.748%) for scour depth and silting height respectively.

Fig. 2 presents the relationship between the outputs of the experimental and numerical models from the scour depth and silting height point of view.

The experimental results were used for developing the following empirical formulae (using statics software program) for the considered bed material.

$$d_{sc}/y = -1.99\ \mathrm{Fr}_{avr.cont.} - 0.842(L/B) - 7.527 \times 10^{-4}\theta + 0.402 \quad (4)$$

(a) Straight Groin (b) Repelling Groin (c) Attracting Groin

Figure 1 Types of groins according to action on flow.

Table 1 Geometry of scour and silting.

Run name	Scour				Silting			
	Measured depth (m)	Predicted depth (m)	Measured width (m)	Measured length (m)	Measured height (m)	Predicted height (m)	Measured width (m)	Measured length (m)
$10S_{10}$	−0.045	−0.043	0.090	0.140	0.012	0.013	0.140	0.140
$20S_{10}$	−0.070	−0.065	0.160	0.250	0.035	0.032	0.190	0.450
$30S_{10}$	−0.080	−0.082	0.185	0.310	0.040	0.041	0.220	0.600
$10S_{15}$	−0.038	−0.040	0.110	0.130	0.012	0.011	0.110	0.160
$20S_{15}$	−0.094	−0.090	0.199	0.232	0.058	0.060	0.261	0.326
$30S_{15}$	−0.095	−0.100	0.280	0.340	0.040	0.036	0.300	1.320
$10S_{20}$	−0.029	−0.032	0.146	0.133	0.024	0.026	0.206	0.217
$20S_{20}$	−0.059	−0.062	0.279	0.332	0.060	0.062	0.344	0.496
$30S_{20}$	−0.109	−0.102	0.333	0.410	0.054	0.052	0.550	1.400
$10A_{10}$	−0.030	−0.031	0.085	0.145	0.013	0.014	0.100	0.140
$20A_{10}$	−0.040	−0.042	0.135	0.190	0.032	0.033	0.130	0.235
$30A_{10}$	−0.060	−0.055	0.150	0.300	0.050	0.045	0.230	0.600
$10A_{15}$	−0.030	−0.029	0.130	0.170	0.017	0.019	0.145	0.170
$20A_{15}$	−0.047	−0.049	0.170	0.280	0.034	0.033	0.200	0.280
$30A_{15}$	−0.075	−0.079	0.200	0.470	0.045	0.041	0.255	0.330
$10A_{20}$	−0.037	−0.042	0.136	0.187	0.034	0.035	0.142	0.195
$20A_{20}$	−0.074	−0.080	0.237	0.468	0.085	0.090	0.237	0.445
$30A_{20}$	−0.085	−0.082	0.300	0.600	0.077	0.079	0.380	1.180
$10R_{10}$	−0.060	−0.057	0.025	0.040	0.035	0.032	0.030	0.080
$20R_{10}$	−0.048	−0.050	0.120	0.180	0.026	0.029	0.140	0.180
$30R_{10}$	−0.060	−0.055	0.145	0.210	0.032	0.033	0.180	0.360
$10R_{15}$	−0.023	−0.026	0.075	0.090	0.010	0.009	0.080	0.120
$20R_{15}$	−0.057	−0.052	0.150	0.280	0.048	0.051	0.190	0.210
$30R_{15}$	−0.095	−0.100	0.210	0.450	0.037	0.034	0.250	0.900
$10R_{20}$	−0.030	−0.033	0.120	0.160	0.020	0.019	0.150	0.140
$20R_{20}$	−0.060	−0.055	0.210	0.400	0.050	0.055	0.250	0.320
$30R_{20}$	−0.110	−0.120	0.250	0.480	0.045	0.042	0.400	0.850
Aver.	−0.061	−0.061	0.171	0.273	0.055	0.053	0.215	0.439

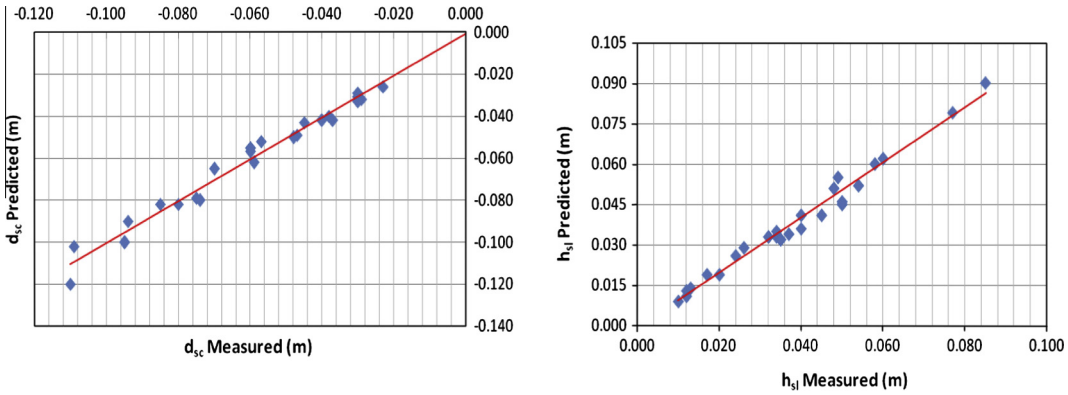

Figure 2 Comparison between measured and predicted scour depths and silting heights.

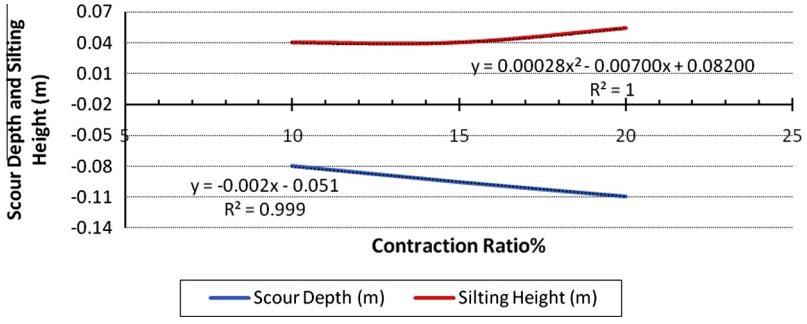

Figure 3 Influence of groin length on scour depth and silting height.

The correlation factors (R^2) = 0.776. The Standard Error of Estimation (SEE) = 0.084.

$$W_{sc}/y = 4.72\ \mathrm{Fr}_{avr.cont} + 5.87(L/B) - 2.26 \times 10^{-3}\theta - 0.971 \quad (5)$$

The correlation factors (R^2) = 0.823. The Standard Error of Estimation (SEE) = 0.206.

$$L_{sc}/y = 11.355\ \mathrm{Fr}_{avr.cont} + 9.88(L/B) - 5.69 \times 10^{-3}\theta - 2.646 \quad (6)$$

The correlation factors (R^2) = 0.893. The Standard Error of Estimation (SEE) = 0.318.

$$h_{sl}/y = \exp(55.394\mathrm{Fr}_{avr.cont} - 40.12(L/B) - 9.99 \times 10^{-2}\theta - 9.182) \quad (7)$$

The correlation factors (R^2) = 0.851. The Standard Error of Estimation (SEE) = 0.278.

$$W_{sl}/y = \exp(4.371\mathrm{Fr}_{avr.cont} + 4.34(L/B) - 2.85 \times 10^{-4}\theta - 1.69) \quad (8)$$

The correlation factors (R^2) = 0.835. The Standard Error of Estimation (SEE) = 0.233.

$$L_{sl}/y = \exp(10.481\mathrm{Fr}_{avr.cont} + 3.52(L/B) - 7.61 \times 10^{-4}\theta - 2.81) \quad (9)$$

The correlation factors (R^2) = 0.71. The Standard Error of Estimation (SEE) = 1.574.

It should be mentioned that the velocity profiles and values at different cross-sections are found at Ibrahim [11].

5.1.1. Influence of groin length on geometry of scour and silting

Figs. 3–5 illustrate the relationship between the groin length and the geometry of scour and silting. The figures were plotted under a fixed maximum discharge and straight groin (i.e. Q = 30 l/s, and θ = 90°). The figures illustrated that the local geometry of scour and silting was directly proportional to the groin length. That agreed with what obtained by Fang et al. [18] and Attia et al. [22].

Moreover, for fixed groin length the scour depth is found to be approximately twice times the silting height. Consequently, a special attention should be provided during the design processes of groin footings to be protected from the risk of failure by scour action. The short groin showed no considerable differences in scour and silting widths. However, the silting width was 65% greater than scour width in case of long groin. The influence of groin length on scour length was limited in comparison with silting length.

5.1.2. Influence of groin orientation angle on geometry of scour and silting

Figs. 6–8 illustrate the influence of groin alignment on the geometry of scour and silting. The figures were plotted under fixed maximum discharge and longest groin length (i.e., Q = 30 l/s and L = 8 cm)

The figures show that for the repelling groin, the maximum scour depth and minimum silting height were located. On the contrary, the attracting groin produced minimum scour depth

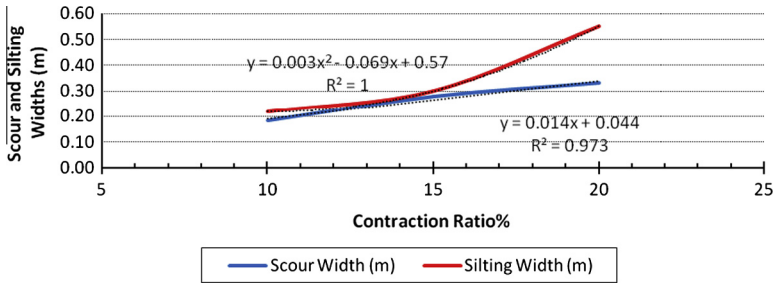

Figure 4 Influence of groin length on scour and silting widths.

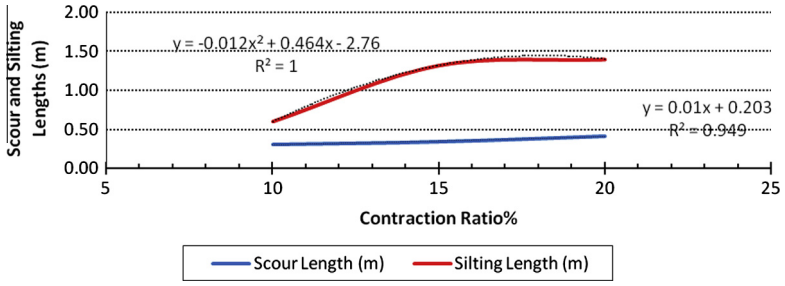

Figure 5 Influence of groin length on scour and silting lengths.

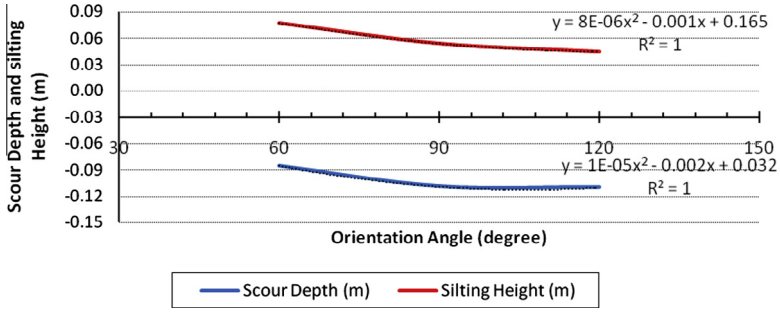

Figure 6 Influence of orientation angle on scour depth and silting height.

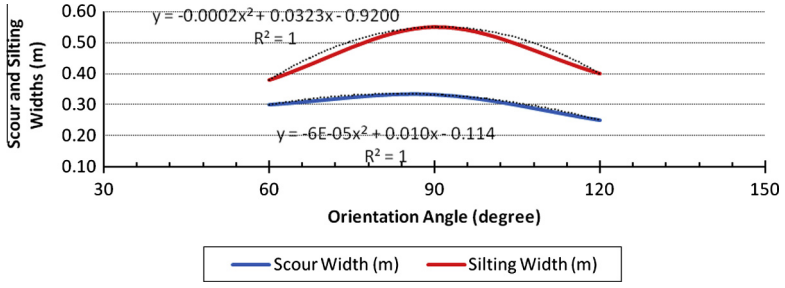

Figure 7 Influence of orientation angle on scour and silting widths.

and maximum silting height. Consequently, it is concluded that the orientation angle was directly proportional to scour depth and inversely proportional silting height. Also, for the same angle it is noticed that the effect of orientation angle on scour depth is higher than silting height.

The maximum scour and silting widths were found at right angled groin. Moreover, the repelling groin showed scour width shorter than the attracting groin. Also, except the right angled groin, the angle influence on silting width is vanished.

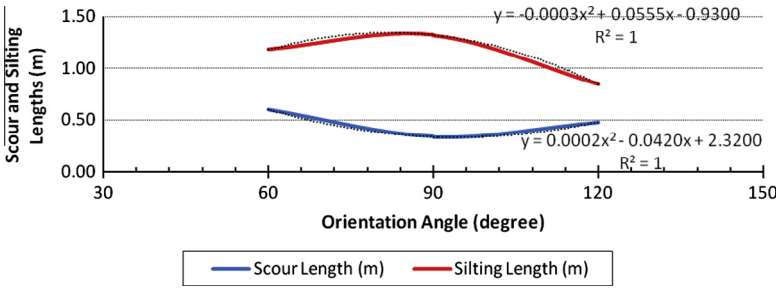

Figure 8 Influence of orientation angle on scour and silting lengths.

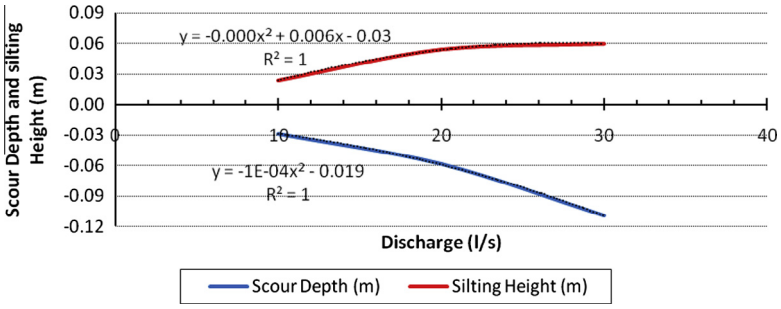

Figure 9 Influence of discharge on scour depth and silting height.

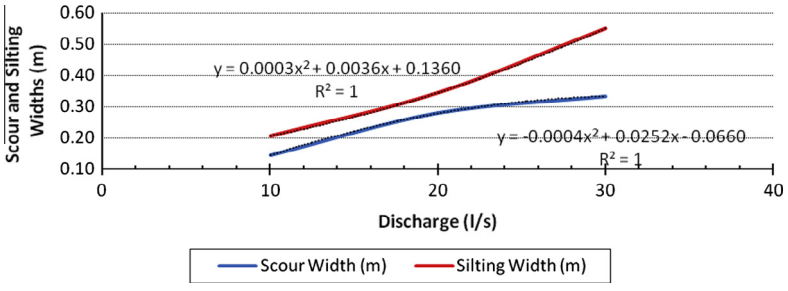

Figure 10 Influence of discharge on scour and silting widths.

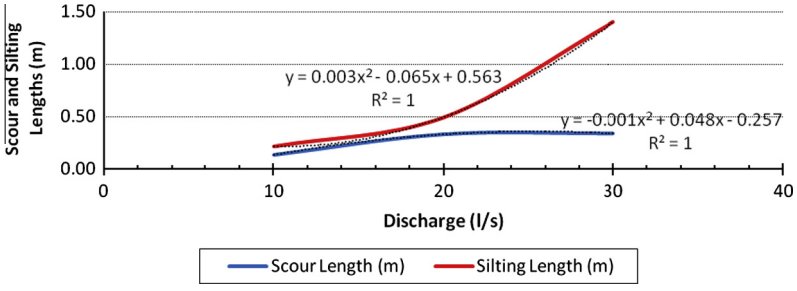

Figure 11 Influence of discharge on scour and silting lengths.

Discussing scour and silting lengths, it is noticed that the right angled groin presented the maximum silting the minimum scour lengths. However, the repelling groin gave shorter scour and silting lengths than the attracting.

5.1.3. Influence of discharge on geometry of scour and silting

Figs. 9–11 present the discharge influence on the geometry of scour and silting. The figures were plotted under fixed right angled groin and maximum groin length (i.e. $\theta = 90°$, and $L = 8$ cm). The figures illustrate that, for the considered discharges, the geometry of scour and silting was directly proportional to the discharge. Also, it is noticed that gap in values between scour and silting increases as the discharge increase.

Fig. 12 presents photos for some tests carefully selected to present the influence of orientation angle on the geometry of local scour resulted in groin existence. The photos are for $30S_{20}$, $30A_{20}$, and $30R_{20}$ respectively.

Figure 12 Geometry of local scour and silting for $30S_{20}$, $30A_{20}$, and $30R_{20}$.

6. Conclusions

The experimental and numerical study of the influence of groin length, orientation angle, and discharge on the geometry of local maximum scour and silting associated to groin installation, led to the following conclusions:

- The groin length showed a significant influence on formation the geometry of bed topography in groin field; however the orientation angle and discharge showed less influence.
- The scour and silting parameters were directly proportional to the groin length and the discharge.
- The orientation angle was directly proportional to scour depth, and inversely proportional to silting height.
- Installing groin at right angles gave maximum scour width and minimum scour length.
- Installing groin at right angles gave maximum silting width, and length.
- Installing long, right angled groin can be used for navigational purposes as the maximum scour depth was found.
- Short attracting or repelling groins can be used for the purposes of bank protection for distances depending on groin length.

For a further evaluation of possible groin designs and their influence on bed morphology, more aspects to be considered with orientation angles like groin permeability, width, submergence, and layout.

Acknowledgements

This work was carried out at the Hydraulics Research Institute (HRI), National Water Research Center (NWRC), Egypt. The author gratefully acknowledges the collaboration done by all staff members of the Institute during the experimental work. Special thanks to Dr. Fahmy S. Abdalhalim for his support and valuable advises.

References

[1] Klingeman PC, Kehe SM, Owusu YA. Stream bank erosion protection and channel scour manipulation using rock fill dikes and gabions. Rep. No. WRRI-98. Corvallis, Ore: Water Resources Research Institute, Oregon State Univ.; 1984.
[2] Shields Jr FD, Cooper CM, Knight SS. Experiment in stream restoration. ASCE J Hydraul Eng 1995;121(6):494–502.
[3] Kuhnle RA, Alonso CV, Shields Jr FD. Geometry of scour holes associated with 90 spur dikes. ASCE J Hydraul Eng 1999;25(9):972–8.
[4] Ohmoto T, Hirakawa R. Secondary current structure in open-channel flow with aeries of submerged groyns. In: Proc. of 12th congress of APD-IAHR, vol. 1. Bangkok; 2000. p. 189–99.
[5] Elawady E, Michiue M, Hinokidani O. An investigation of scour around attracting spur-dikes. Advances in fluid modeling and turbulence measurements. In: Proc. of 8th Intr.; 2002.
[6] Elawady E, Michiue M, Hinokidani O. Characteristics of scour around repellingspur-dikes. In: Proc. of 29th congress of IAHR. Beijing: Theme D, II; 2001. p. 343–49.
[7] Tominaga A, Nagao M, Nezu I. Flow structure and mixing processes around porousand submerged dikes. In: Proc. of 27th congress of IAHR. San Francisco: Theme B, 1; 1997. p. 251–56.
[8] Uittewaal WSJ, Berg MH. Experiments on physical scale models for submergedand non-submerged groins of various types. In: Bousmar and Zech, editors. River Flow 2002; 2002. p. 1377–383.
[9] Uittewaal WSJ, Lehmann D, Mazijk A. Exchange processes between a river and its groin field: model experiments. ASCE J Hydraul Eng 2001;127(11):928–36.
[10] Abdelmageed. The effect of inclined groins on the flow. Int J Water Resour Environ Eng 2011;3(8):167–75.
[11] Ibrahim M. Experimental study to investigate the flow pattern associated to angled groins. J Am Sci 2012;8(10):313–22.
[12] Vaghefi M, Ghodsian M, Neyshabouri S. Experimental study on scour around a T-shaped spur dike in a channel bend. ASCE J Hydraul Eng 2012;138(5):471–4.
[13] Jamieson E, Rennie C, Townsend R. 3D flow and sediment dynamics in a laboratory channel bend with and without stream barbs. ASCE J Hydraul Eng 2013;139(2):154–66.
[14] Jamieson E, Rennie C, Townsend R. Turbulence and vortices in a laboratory channel bend at equilibrium clear-water scour with and without stream barbs. ASCE J Hydraul Eng 2013;139(3):259–68.
[15] Huthoff F, Pinter N, Remo J. Theoretical analysis of wing dike impact on river flood stages. ASCE J Hydraul Eng 2013;139(5):550–6.
[16] Ali S, Uijttewaal W. Flow resistance of vegetated weir like obstacles during high water stages. ASCE J Hydraul Eng 2013;139(3):325–30.
[17] Uijttewaal W. Effects of groyne layout on the flow in groyne fields: laboratory experiments. ASCE J Hydraul Eng 2004;131(9):782–91.
[18] Fang H, Bai J, Guojian H, Zhao H. Calculations of non-submerged groin flow in a shallow open channel by large eddy simulation. ASCE J Eng Mech. [posted ahead of print September 20, 2013].
[19] Sukhodolov A, Engelhardt C, Kruger A, Bungartz H. Case study: turbulent flow and sediment distributions in a groyne field. ASCE J Hydraul Eng 2004;130(1):1–9.
[20] Maleki H, Chenari S, Selahshour J, Zand F. Three-dimensional simulation of flow and vortex patterns around the L-shaped impermeable groins at five different angles of the first half of the semicircular arc. Tech J Eng Appl Sci 2013;3(9):727–31.
[21] Naghshine M, Shooshtari M, Kashkuli H, Hasoonizade H. Studying the effects of groin on controlling the sediments entering the intake branching from a 180° bend. Int J Agric Crop Sci 2013;5(23):2899–905.

[22] Attia K, Talaat A, Elsaeed G, Ibrahim M. Local scour as a result of spur dike implementations. Nile Water Sci Eng J 2010;3(3):62–72.
[23] Molinas A, Hafez YI. Finite element surface model for flow around vertical wall abutments. J Fluid Struct 2000;14:711–33.
[24] Ibrahim M. Hydrodynamic behavior of bank protection structures (Groins). Thesis Submitted to Faculty of Engineering. Benha University for partial Fulfillment of the Requirements for Master Degree of Science in Civil Engineering, Egypt; 2005.

Dr. Mohammad Mahmoud Ibrahim. Dr.Ibrahim is working as a lecturer in civil engineering department, Shoubra faculty of engineering, Benha University. He has a broad experience, covering the different aspects of hydraulic, and harbor engineering; his professional experience in the sphere river and hydraulic structures studies, executing power plants, barrages studies, teaching national scientific courses in Egypt, published researches in the field of specialization, supervising master of science and doctoral researchers and technical report writing in both English and Arabic languages.